Biol. Cybern. (2005) 92: 367–379
DOI 10.1007/s00422-005-0565-z

ORIGINAL PAPER

Biological Cybernetics

**Robert Kozma · Marko Puljic · Paul Balister
Bela Bollobás · Walter J. Freeman**

# Phase transitions in the neuropercolation model of neural populations with mixed local and non-local interactions

Received: 1 November 2004 / Accepted: 18 March 2005 / Published online: 25 May 2005


**Abstract** We model the dynamical behavior of the neuropil, the densely interconnected neural tissue in the cortex, using neuropercolation approach. Neuropercolation generalizes phase transitions modeled by percolation theory of random graphs, motivated by properties of neurons and neural populations. The generalization includes (1) a noisy component in the percolation rule, (2) a novel depression function in addition to the usual arousal function, (3) non-local interactions among nodes arranged on a multi-dimensional lattice. This paper investigates the role of non-local (axonal) connections in generating and modulating phase transitions of collective activity in the neuropil. We derived a relationship between critical values of the noise level and non-locality parameter to control the onset of phase transitions. Finally, we propose a potential interpretation of ontogenetic development of the neuropil maintaining a dynamical state at the edge of criticality.

## 1 Introduction

The emergence of collective behaviors in chaotic systems were studied extensively using various cellular automata and lattice models. The results indicated that low-dimensional structure and collective oscillations may arise on the macroscopic level in a system with extensively chaotic components at the microscopic level (Aihara et al. 1990; Kaneko 1990; Pomeau 1993; Marcq et al. 1997). The significance of intermediate-range or mesoscopic effects has been outlined in further studies, with a special emphasis on neurodynamics (Kozma 1998; Freeman 1999). Random cellular automata (RCA) appear to have many of the features of these systems, but are simpler to describe, easier to simulate, and are more amenable to rigorous analysis. The present paper concentrates on applying and generalizing the concept of RCA for the description of the dynamics of neural populations.

The theory of random cellular automata is closely related to that of percolation theory, which was an active area of research in the past decades. Percolation theory lies at the interface of probability theory, combinatorics, and physics (Stauffer and Aharony 1994, Grimmett 1999). Interest in various aspects of standard percolation remains high, including estimates of critical probabilities (Bollobás 1985; Balister et al. 1993). Recently, more and more modifications of the standard percolation models were studied. In particular, there has been much work on the family of processes know as bootstrap percolation (Aizeman and Lebowitz 1988; Duarte 1989; Gravener and McDonald 1997; Cerf and Cirillo 1999). Computer experiments have suggested interesting non-trivial large-scale behavior, and many deep mathematical results were proved about a number of models. Percolation theory deals with large-scale properties of certain types of random graphs, often built on d-dimensional lattice $Z^d$.

In the archetypal percolation problem, the vertices (sites) are the points of a lattice with edges (bonds) joining neighboring sites. In site percolation, sites are open independently with probability $p$ and one wishes to answer questions about the size of the connected components formed by these open sites. In particular, do infinite connected clusters of open sites exist? Similar questions can also be asked about bond percolation, where the bonds are chosen to be open with a certain probability. There are many variants of these problems. For example, in oriented percolation, one asks for infinite paths of connected open sites that travel at each step only in certain directions.

Many percolation problems exhibit phase transitions. In the case of phase transitions, for $p$ less than some critical probability $p_{\text{crit}}$ only finite clusters exist, and for $p > p_{\text{crit}}$

R. Kozma (✉), M. Puljic, P. Balister, B. Bollobás
Department of Mathematical Sciences,
University of Memphis Memphis,
TN 38152, USA
e-mail: rkozma@memphis.edu,
URL: http://cnd.memphis.edu

W. J. Freeman
Division of Neurobiology,
University of California at Berkeley
Berkeley, CA 94720, USA
wfreeman@socrates.berkeley.edu,
URL:http://sulcus.berkeley.edu

infinite clusters almost surely exist (Grimmett 1999). Random automata are also closely related to certain models in statistical physics such as the Ising model. This naturally leads to questions about phase transitions and their associated critical exponents which describe the properties of systems that are close to a phase transition. Studying phase transitions gains increasing popularity in various research fields beyond physics, including population dynamics, the spread of infectious diseases, social interactions, and computer networks (Kauffman 1990; Crutchfield 1994; Haken 1999; Watts and Strogatz 1998; Newman 2000). In the realms of neuropercolation we extend percolation theory to study neural processes (Kozma et al. 2001, 2004).

Recent studies explain spatial patterns of phase in beta–gamma EEG activity of human neocortex (Freeman 2003b,c). Neocortex maintains a stable, scale-free state by homeostatic regulation of neural firing, through which it adapts instantly and globally to rapid environmental changes. The coherent states created by the destabilization of the cortex are called 'wave packets' (Freeman 2003a). Destabilization is initiated at a given, seemingly random point of time and space on the cortex. This resembles phase transition in physical systems, which start at a certain nucleus.

EEG analysis gave spatiotemporal amplitude modulation (AM) patterns of unprecedented clarity (Freeman, 2004) and supported the theory of self-organized criticality in neural dynamics (Bak et al. 1987; Bak 1996; Jensen 1998). Spatial gradients of beta–gamma phase revealed multiple co-existing phase patterns that were consistent with a state of self-organized criticality. These results indicate that brains maintain themselves at the edge of global instability by inducing a multitude of small and large adjustments. Each adjustment is a sudden and irreversible change in the state of a neural population. Because sensory cortices maintain themselves in highly sensitive meta-stable states, they can transit instantly to any designated part of their state space when destabilized by expected stimuli.

Synchronization of neural electrical activity while completing cognitive tasks is studied in various animals, e.g., cats, rabbits, gerbils, macaque monkeys (Barrie et al. 1996; Ohl et al. 2001, 2003; Freeman 2003a; Bressler 2003). It was demonstrated that using an animal model of category learning, the sorting of stimuli into these categories emerges as a sudden change in the animal's learning strategy. EEG and ECG recordings show that the transition is accompanied by a change in the dynamics of cortical stimulus representation, which represent a mechanism underlying the recognition of the abstract quality (or qualities) that defines the categories. Synchrony of firing of widely distributed neurons in large numbers is necessary for emergence of spatial structure in cortical activity by reorganization of unpatterned background activity.

Oscillations measured by EEG, MEG, and other brain-monitoring techniques arise from extensive feedback interactions among neurons densely connected in local neighborhoods, in combination with the effects of long axons. Axonal effects have high conduction velocities and support synchronization over large areas of cortex (Bressler and Kelso 2001; Bressler 2002; Freeman 2004), creating small-world effects (Watts and Strogatz 1998; Wang and Chen 2003) in analogy to the rapid dissemination of information through social contacts. Small-world networks have certain preferential attachment rules between vertices that make the network diameter much smaller than regular ones, like grids and lattices. The importance of long-distance correlations was emphasized by numerous brain theorists (e.g., (Ingber 1995; Hoppensteadt and Izhikevich 1998; Haken 1999; Friston 2000; Linkenkaer et al. 2001; Kaneko and Tsuda 2001; Kozma et al. 2004; Stam et al. 2003). In certain networks, like the www, biological systems, the degree distribution follows a power law, i.e., it is scale-free. Crucial developments were reported concerning scale-free networks (Albert and Barabási 2002; Barabási and Bonabeau 2003; Bollobás and Riordan 2003).

Neuropercolation approach has some common aspects with small-world and scale-free network studies. However, key differences have to be pointed out. While scale-free network studies strongly rely on the established methods of statistical physics, neuropercolation goes beyond existing tools. The neural tissues in the brains, called neuropil, have unique properties requiring not just new models, but completely new mathematical methods of thorough analysis. Neuropercolation is a generalization of cellular automata, Hopfield memory arrays and Conway's game of life (Hopfield 1982; Berlekamp et al. 1982), by merging the concepts of random graph theory (Erdős and Rényi 1960; Bollobás 1985) and non-local interactions represented by axonal connections. It bridges the gap between Ising-type models and mean-field approaches (Kozma et al. 2003; Balister et al. 2004). Our studies identify several key factors that determine phase transitions in our neural models, including endogeneously generated noise and the structure and extent of the non-locality of neural populations. The resulting novel tools were used to study the intricate complexity of dynamic behaviors of neural populations (Puljic and Kozma 2003, 2005).

The present paper starts with the description of basic principles and formalism of neuropercolation. We introduce results of mean field models as well as locally connected RCA lattices. Next, the critical behavior in mixed local and non-local models is described. We build phase diagrams to characterize the relationship between critical noise and extent of non-locality. This is followed by the characterization of a potential developmental process in brain after birth and early childhood, which may be responsible for maintaining dynamical state of brains at the edge of criticality.

## 2 Overview of phenomenology of neuropercolation

### 2.1 Role of dynamics in neural populations

We model the dynamical behavior of the neuropil, the densely interconnected neural tissue in the cortex. Most synaptic activity in the brain occurs in the neuropil. Neuropil is a unique

felty substance, believed to be one of the most highly organized in the Universe. It represents a complicated spatial network comprising interconnected neuronal processes intermingled with irregularly shaped processes of astrocytic glia (Peters et al. 1991). Neural populations stem ontogenetically in embryos from aggregates of neurons that grow axons and dendrites and form synaptic connections of steadily increasing density. At some threshold, the density allows neurons to transmit more pulses than they receive, so that an aggregate undergoes a state transition from a zero point attractor to a non-zero point attractor, thereby becoming a population. Interacting excitatory and inhibitory populations produce periodic, limit cycle oscillations. Dopamine induced bistability may play an important role in shaping oscillations in the neuropil (Gruber et al. 2003). At the next level of complexity, an increasing volume of research aims at the interpretation of dynamic brain activity in terms of aperiodic, chaotic processes (Skarda and Freeman 1987; Schiff 1994; Arhem et al. 2000; Dafilis et al. 2001; Korn and Faure 2003).

A chaotic system has the capacity to create novel and unexpected patterns of activity. It can jump instantly from one mode of behavior to another. It retains in its pathway across its basins a history, which fades into its past, just as its predictability into its future decreases. A chaotic time series does not converge to a fixed point, limit cycle, or hyper torus. It lacks constant frequencies but has a spectral domain with peak frequencies. In EEG signals, we define a chaotic attractor as a region of the phase space in which the system is constrained for several cycles of the peak frequencies, and to which it can return after it is displaced by a perturbation. We define a state transition as a passage across a separatrix from one attractor to another as the trajectory crosses a landscape of attractors. There are multiple landscapes, and a phase transition is defined as the activation of by input of an attractor landscape, from which the input selects the basin of one attractor. This process underlies perceptual categorization. Transitions between chaotic states constitute the dynamics that explains how brains perform such remarkable feats as abstraction of the essentials of figures from complex, unknown and unpredictable backgrounds, generalization over examples of recurring objects, reliable assignment to classes that lead to appropriate actions, planning future actions based on past experience, and constant updating by way of the learning process (Freeman 1999).

In this paper, we explore several directions of the generalization of the basic concept of phase transition in random graphs, including random transition effects and non-local interactions. Presently, only a very few simple models allow a strict mathematical treatment and proof of the existence of phase transitions in generalized systems (Balister et al. 2003, 2004). Large part of the results described here are based on extensive numerical computations. It is to be emphasized that the models introduced in this work represent the very first basic building blocks of neurodynamics, namely, the generation of neural populations with non-zero attractors (Freeman 1975). The present work contains crucial results, which are necessary to firmly establish the foundations of practically useful computational models of phase transitions, in the style of brains. Modeling high-level cognitive processing, like abstraction and generalization, which were described previously as transitions between chaotic states, is well-beyond the goals of this study.

### 2.2 Random cellular automata formalism

General models of random cellular automata (RCA) are well-documented, see (Toom et al. 1990; Gács 1990; Maes and Vande Velde 1997; and others). Here we limit our discussions to a model on the 2-dimensional lattice $Z^2$. Let $x = \{i, j\}$ is a site in $Z^2$. The activation of site $x$ at time $t$, $a_x(t)$, can be 0 or 1. The fate of each site will be influenced by the sites in the neighborhood $\Lambda(x)$. Introduce $s(x)$ as the arousal function and $r(x)$ as the depression function. The arousal function gives the probability that an inactive site becomes active, while the depression function is the probability that an active site becomes inactive at the next step. At time 0, the sites are active with probability $p$. At each time step $t$, every site is updated simultaneously according to the rules:

$$s(x) = \{\varepsilon_1, \quad \text{if } C_t; \quad 1-\varepsilon_1 \quad \text{if } \neg C_t\}, \tag{1}$$

$$r(x) = \{\varepsilon_2, \quad \text{if } \quad C_t\ ; \quad 1-\varepsilon_2 \quad \text{if } \neg C_t\}. \tag{2}$$

Here we introduced event $C_t$ as follows:

$$C_t : \sum_{k\in\Lambda(x)} a_k(t) \le \frac{|\Lambda(x)|}{2} \tag{3}$$

$C_t$ means that the majority of sites in the neighborhood $\Lambda(x)$ are inactive at time $t$. Here $|\Lambda(i, j)|$ denotes the cardinality of neighborhood $\Lambda(i, j)$. For example, in a 2-dimensional lattice with local interactions, we have $|\Lambda(i, j)| = 5$, when self-connection is included.

In the case when no cell can change from active to inactive ($r(x) = 0$ for all $x$), we recover the bootstrap percolation model. Clearly, the family of random cellular automata is much richer than the family of bootstrap percolations. In particular, if all the probabilities are 0 or 1, we recover the theory of deterministic cellular automata, such as that of Conway's Game of Life (Berlekamp et al. 1982). These models are known to be capable of producing extremely complex behavior. On the other hand, if we choose $j(x)$, $r(x) \neq 0$, 1 for all $x$, then there is no need for an initial probability p, and with a suitable choice of the arousal and depression functions, we may achieve that the system hovers around a certain density of active sites.

### 2.3 Mean field random cellular automata models

Phase transitions in mean field random cellular automata models are analyzed in details by (Balister et al. 2003). Here we summarize the results for the case of a finite grid or torus $Z_n^2$. In the mean field model instead of taking $|\Lambda|$ specified neighbors, we take $|\Lambda|$ elements of the grid at random with replacement. It is clear that the mean field model does not

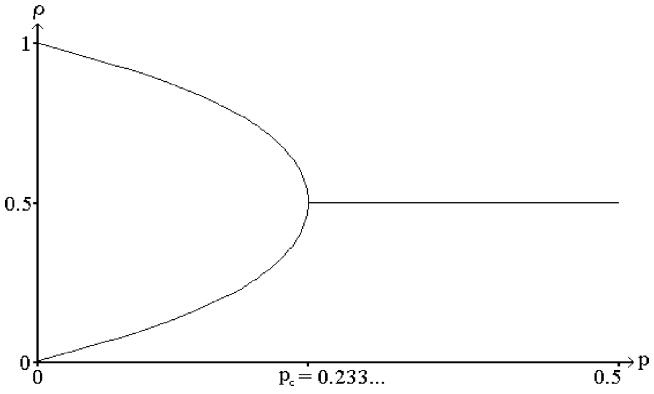


**Fig. 1** Stable density $\rho$ of the mean field model; critical probability $p_c = 0.233$

depend on the topology of the grid, and the only information of relevance is the cardinality

$$X_t = \sum_{k \in Z_n^2} a_k(t). \tag{4}$$

We define $\rho_t$ to be $X_t/N$ where $N = n \times n$ is the size of the finite grid or torus. Thus, $\rho_t \in [0, 1]$ gives the density of active points.

Let us consider the symmetric model $s = 1-r$. It is readily shown that the mean field model in this case has one fixed point at $\rho = 0.5$ for $\varepsilon \in [\varepsilon_c, 0.5]$, but for $\varepsilon < \varepsilon_c$, the fixed point $\rho = 0.5$ is unstable and there are two other fixed points which are stable (Balister et al. 2004). Here we illustrate the results in the 2-dimensional lattice, where the critical probability $\varepsilon_c = 7/30$. Indeed, let us write the condition for the fixed point density as:

$$d = (1-\varepsilon)\left(\sum_{i=0}^{\lfloor |\Lambda|/2 \rfloor} B(|\Lambda|, i) d^{|\Lambda|-i}(1-d)^i\right) + \varepsilon\left(1 - \sum_{i=0}^{\lfloor |\Lambda|/2 \rfloor} B(|\Lambda|, i) d^{|\Lambda|-i}(1-d)^i\right), \tag{5}$$

where $B(a, b)$ is the binomial coefficient. Considering $|\Lambda| = 5$, one readily obtains the condition for stable solution as $\varepsilon_c = 0.5 - (12d^4 - 24d^3 + 8d^2 + 4d + 2)^{-1}$. After substituting the value $d = 0.5$ at criticality, we get $\varepsilon_c = 7/30$. The above equation describing the fixed points approximates power law relationship with very good accuracy:

$$|d - 0.5| \propto (\varepsilon_c - \varepsilon)^{\beta}, \tag{6}$$

where $\beta \approx 0.5$. Figure 1 illustrates the stable density values for $0 \le \varepsilon \le \varepsilon_c$ as described by the above equation.

## 2.4 Local majority percolation models

Theoretical description of phase transitions in local RCA is a very difficult problem. Mathematical description of phase transitions in a narrow class of RCA with $\varepsilon \approx 0$ are given in (Balister et al. 2004). Namely, we gave a rigorous proof of the fact that the model spends a long time in either low- or high-density configurations before crossing very rapidly to the other state. Fairly good bounds were proved on the very long time the model spends in the two essentially stable states and on the very short time it takes to cross from one essentially stable state to another. This result, in fact, gives a theoretical justification of the terminology 'neuropercolation' of our approach. It is expected that these results can be generalized to a wider range of $\varepsilon$. However, conditions near the critical regime of RCAs are not tractable by rigorous mathematical methods at present.

**Table 1** Comparison of RCA and Other Lattice Models

| | $\beta$ | $\gamma$ | $\nu$ | $I_{\text{error}}$ |
|---|---|---|---|---|
| RCA[1] | 0.1308 | 1.8055 | 1.0429 | 0.02 |
| TCA[2] | 0.12 | 1.59 | 0.85 | 0.13 |
| Ising(2D)[3] | 0.125 | 1.75 | 1 | - |
| CML [4] | 0.115 | 1.55 | 0.89 | 0.00 |

(1) Kozma et al. (2003), (2) Makowiec (1999); (3) Cipra (1987); (4) Marcq et al. (1997)

In the following discussions, we use extensive numerical simulations to study the critical behavior of the neuropercolation model. Simulations were run on a 2-dimensional torus $Z_n^2$ of size up to $256 \times 256$. The next state of the site at a given location will be given by the majority of the states of itself and its four nearest neighbors, see Eqs.(1, 2, 3). All the sites will be updated simultaneously at a certain time $t$. At any time instant, the average activation $\rho(t)$ was calculated as the mean value over all lattice points, which is analogous to the magnetization parameter of Ising models (Makowiec 1999).

As we vary $\varepsilon$ in the range $[0, 0.5]$, the model exhibits a behavior similar to that seen in the mean field model. For small $\varepsilon$ there are two stable states, one with low density $\rho$ and one with high density $1 - \rho$. There is a probability that the system switches between high and low density states. This probability can be made very small by increasing the grid size $n$. For $\varepsilon$ close to the critical probability, one sees large grid regions with high density and large regions with low density evolving in time and space. The variance of the density drastically increases as $\varepsilon \to \varepsilon_c$. An important difference between mean field models and local RCA is that the critical probability is significantly lower in RCA with $\varepsilon_c \approx 0.1342$. For $\varepsilon_c < \varepsilon < 0.5$ the stationary density distribution of $\rho_t$ is unimodal for a sufficiently large but finite lattice. For $\varepsilon < \varepsilon_c$ the distribution becomes bimodal, as one would expect from the mean field model.

In the characterization of RCA, we follow the methodology applied by (Makowiec 1999), based on Binder's finite-size scaling theory (Binder 1981). Details of this methodology will be given in the next section, where models with nonlocal connections are described. Here we summarize the results obtained for the local RCA with majority voting rule. According to finite-size scaling theory, the following power

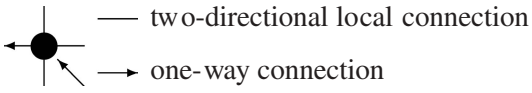


**Fig. 2** Example of an inactive site with local and remote connections

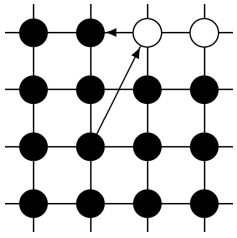

**Fig. 3** Example of a lattice with local and remote connections

laws are expected to hold:

$$\rho \sim (\varepsilon - \varepsilon_c)^{\beta} \quad \text{for } \varepsilon_c \leq \varepsilon \tag{7}$$

$$\chi \sim |\varepsilon - \varepsilon_c|^{-\gamma} \quad \text{for } \varepsilon \to \varepsilon_c \tag{8}$$

$$\xi \sim |\varepsilon - \varepsilon_c|^{-\nu} \quad \text{for } \varepsilon \to \varepsilon_c\,. \tag{9}$$

In the above equations, the following quantities are used: critical probability $\varepsilon_c$, susceptibility $\chi$, and correlation length $\xi$. The estimated values of the critical exponents $\beta$, $\gamma$, $\nu$ are given in Table 1. The results are reproduced from (Kozma et al. 2003), and they are compared with exponents obtained by the 2-dimensional Ising model, Toom cellular automata (TCA) based on (Makowiec 1999), and coupled map lattice model (CML) using (Marcq et al. 1997). For the Ising model, the following identity function holds:

$$2\beta + \gamma = 2\nu\,. \tag{10}$$

Table 1 contains the error of the identity function, which is defined as the difference of the left-hand side and right-hand side of the above equation $I_{\text{error}} = 2\beta + \gamma - 2\nu$. It has been concluded that the RCA with local majority voting satisfies the exponential scaling relationships very well and it belongs to the Ising, or possibly to a weak-Ising universality class (Kozma et al. 2003).

## 3 Critical behavior in mixed models

### 3.1 Definition of mixed models

In the previous discussions, we have introduced simplified models with either mean-field interactions, or RCAs with local neighborhoods in the d-dimensional lattice. In this section, we turn our attention to more realistic models of the neuropil with a mixture of local and non-local connections. In our model, local connections correspond to dendritic interactions in the arbor of the neuron, while non-local connections describe far-reaching effects through long axons. In our treatment, we want to preserve as much as possible from the results obtained previously, in particular, concerning phase transitions. At the same time, we generalize the previous results, to describe better the dynamics of cortical processes.

The mixed model has neurons with local and non-local connections in the 2-dimensional lattice; see Figs. 2 and 3. Starting with a lattice having only local neighborhoods, we add non-local (remote) connections to randomly selected sites. The cardinality of the neighborhood does not change. Accordingly, for each non-local neighbor, we cut a randomly selected local neighbor. The locations of remote connections are fixed and chosen randomly at the initiation. In the updates, we use the majority rule as given by Eqs. (1–3). The local neighborhood of site $x = \{i, j\}$ is given as $\Lambda(\{i, j\}) = \{\{i-1, j\}, \{i+1, j\}, \{i, j\}, \{i, j-1\}, \{i, j+1\}\}$. An example of the neighborhood in case of an additional remote neighbor is: $\Lambda(\{i, j\}) = \{\{i, j\}, \{i, j-1\}, \{i, j+1\}, \{i+1, j\}, \{i+1, j+1\}\}$; see Fig. 2.

### 3.2 Experiments with mixed models

Starting with a lattice with randomly initiated site activation and having a small value of $\varepsilon$, the activity of the network quickly stabilizes in either mostly active or mostly inactive mode of behavior. Because the systems are of finite size, they jump after a sufficiently long time from one mode of behavior to the other.

Examples of temporal dynamics of a system with 5% of the sites having one remote neighbor are shown in Fig. 4. Results are obtained with experiments on $128 \times 128$ lattices for $10^6$ steps. The figures illustrate subcritical ($\varepsilon = 0.146$), critical ($\varepsilon = 0.147$), and supercritical ($\varepsilon = 0.147$) configurations, respectively.

Figure 4 shows that the two modes are symmetrical. As $\varepsilon_c$ increases, jumps between the two stable states become more frequent. Beyond the critical probability $\varepsilon_c$, the oscillations become unimodal and the oscillation intensity decreases.

Figure 5 shows the average densities as the functions of $\varepsilon$ for four typical systems: the systems with no remote neighbors (local), the systems with 25% sites having one remote connection (25% (1)), the systems with 100% sites having one remote connection (100% (1)), and the systems with 100% sites having four remote connections (100% (4)).

Figure 6 shows the typical spatial patterns for various configurations of remote neighbors. We applied three levels of $\varepsilon$ in each configuration. The applied $\varepsilon$ values correspond to subcritical, critical, and supercritical regimes. Let us define the parameter $m(t) = \rho(t) - 0.5$, which can be interpreted as magnetization in our model. The sites were initiated as mostly active. On the left side in Fig. 6, $\varepsilon$ is far below $\varepsilon_c$. In the middle part, $\varepsilon \approx \varepsilon_c$. On the right side of Fig. 6, $\varepsilon$ is greater then $\varepsilon_c$. We can observe that subcritical and supercritical regimes give spatial distributions indicating ferromagnetic and paramagnetic states, respectively, as described by Ising models. In the case of critical noise level (middle column), spatial clustering is apparent, especially for configurations with smaller number of remote connections, i.e., on Fig. 6a and b.

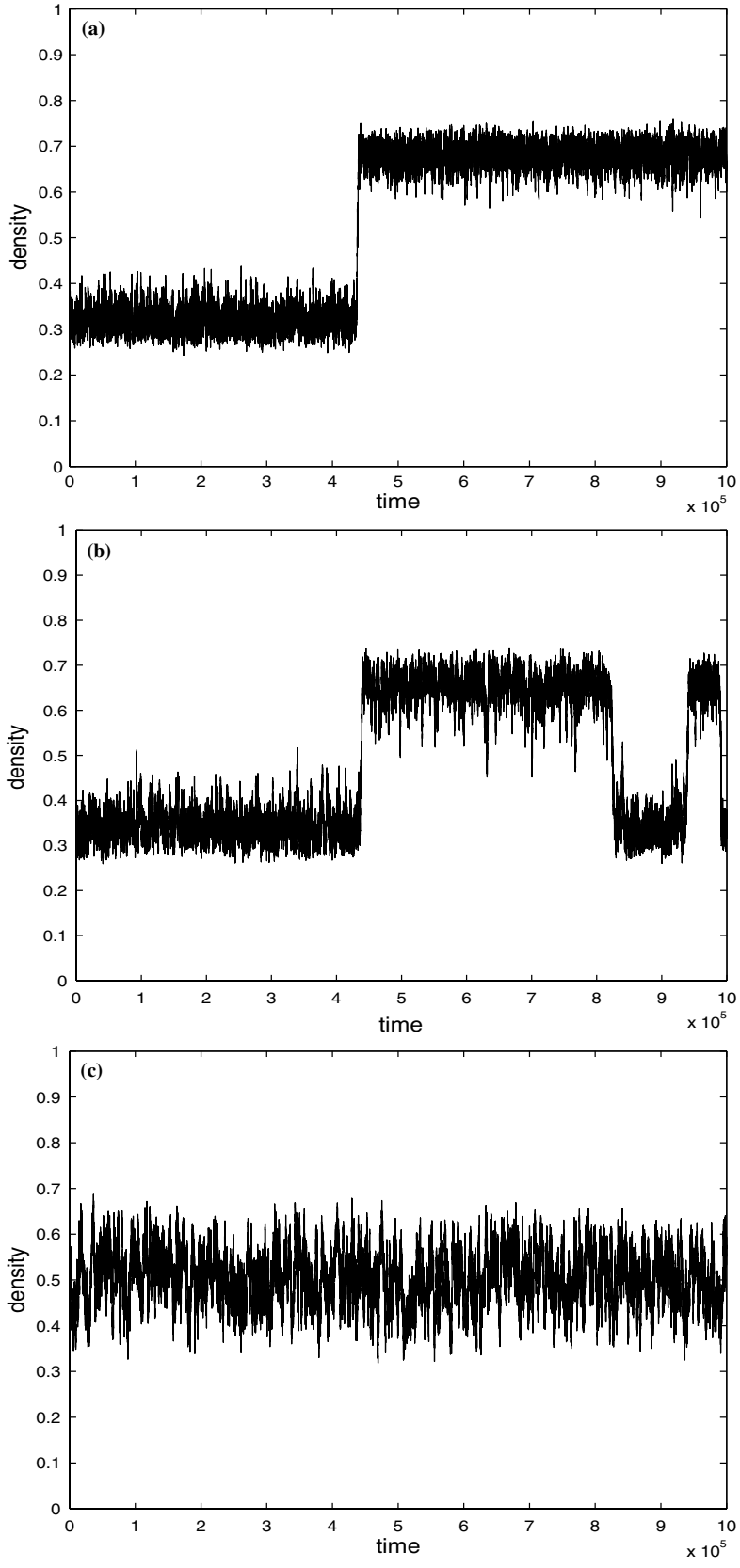


**Fig. 4** Typical temporal behavior of the active sites for $10^6$ steps. 5% of the sites have one randomly selected remote neighbor. Lattice size is $128 \times 128$; **a** $\varepsilon = 0.146$, **b** $\varepsilon = 0.147$, **c** $\varepsilon = 0.151$

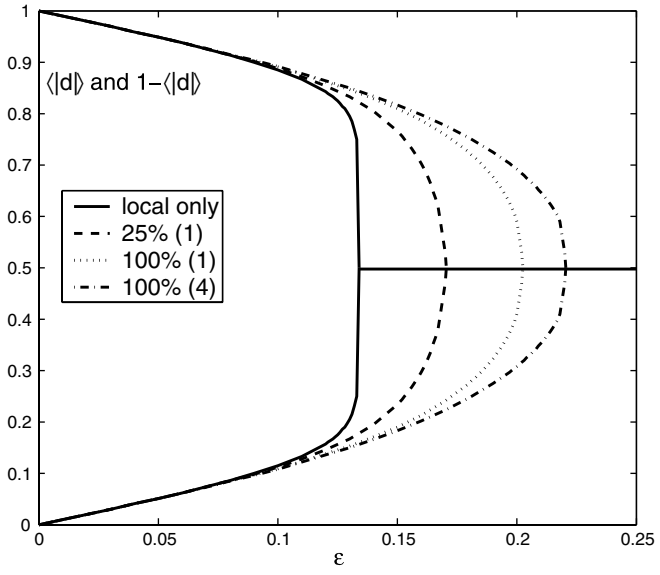


**Fig. 5** Activation density as the function of $\epsilon$ for the systems with no remote neighbors, 25%(1), 100%(1), and 100%(4), respectively

### 3.3 Critical exponents of mixed models

The probability distribution of the density (magnetization) is bimodal for $\varepsilon < \varepsilon_c$. As $\varepsilon$ increases, the peaks of the probability distribution function get closer to each other and its peakedness increases. Measures of the peakedness are given by the kurtosis, the fourth moment of the probability distribution. Peakedness is given by:

$$\alpha_4(\rho) = \frac{\langle(\rho - \langle\rho\rangle)^4\rangle}{\langle(\rho - \langle\rho\rangle)^2\rangle^2}\,. \tag{11}$$

In our model $\langle\rho\rangle = 0.5$. Binder (1981) defines the 4th order cumulants of the magnetization ($m = \rho - 0.5$) as follows:

$$U(l, \epsilon) = 1 - \frac{\langle m^4\rangle}{3\langle m^2\rangle^2}\,. \tag{12}$$

Finite-size scaling theory implies that the interpolated values of Eq. (12) are expected to intersect at a unique point at the critical state, independently of the lattice size, which we denote here as $l$. The location of this intersection will give $\epsilon_c$. Following (Makowiec 1999) we write the scaling equations near the critical point, to obtain scaling exponents $\nu$, $\beta$, and $\gamma$. Exponent $\nu$ describes scaling of the correlation length, and it is obtained from the 4th order cumulant $U(l, \varepsilon)$ as follows:

$$\frac{dU(l, \varepsilon_c)}{d\varepsilon} \propto l^{\frac{1}{\nu}}. \tag{13}$$

For the magnetization, the following relationship holds:

$$\langle|d(l, \varepsilon_c)|\rangle \propto l^{-\beta/\nu}, \tag{14}$$

where the average magnitude of the magnetization is given by:

**Table 2** Critical exponents in mixed models

| | $\varepsilon_c$ | $\beta$ | $\gamma$ | $\nu$ | $I_{\text{error}}$ |
|---|---|---|---|---|---|
| local | 0.1342 | 0.1308 | 1.8055 | 1.0429 | 0.02 |
| 25%(1) | 0.1702 | 0.3071 | 1.1920 | 0.9504 | 0.09 |
| 100%(1) | 0.2032 | 0.4217 | 0.9873 | 0.9246 | 0.02 |
| 100%(4) | 0.2227 | 0.4434 | 0.9371 | 0.9026 | 0.02 |

$$\langle|d|\rangle = \frac{1}{n}\sum_{t=1}^{n}|d(t) - \frac{1}{2}|. \tag{15}$$

Susceptibility $\chi$ is defined as follows:

$$\langle\chi(l, \varepsilon_c)\rangle = l^2(\langle|d(l, \varepsilon_c)|^2\rangle - \langle|d(l, \varepsilon_c)|\rangle^2) \tag{16}$$

Susceptibility $\chi$ satisfies the scaling relationship:

$$\langle\chi(l, \varepsilon_c)\rangle \propto l^{\gamma/\nu - 2}. \tag{17}$$

### 3.4 Estimating critical parameters in mixed models

Experiments were conducted for four different lattice sizes $l = 64, 80, 96$, and 112, respectively. For each lattice size, we have performed experiments with the following lattice configurations: system with no remote connections, and systems with remote connections 25%(1), 100%(1), and 100%(4), i.e, 25% and 100% of sites having one remote neighbor, and 100% of sites having four remote neighbor, respectively. The model with local connections only were introduced in the previous section. Results with mixed configurations are shown in Fig. 7. Simulations were conducted with at least $5 \times 10^7$ steps or until $\langle|0.5 - d|\rangle \leq 0.00005$. Using linear interpolations of the scaling relations in the previous section, we determine the critical exponents for all the systems and configurations. The obtained critical parameters are summarized in Table 2.

The first step is to calculate $\varepsilon_c$; see Fig. 7a, top row. Having $\varepsilon_c$, $\nu$ equals to the slope of linearly interpolated $dU(64, \varepsilon_c)/d\varepsilon$, $dU(80, \varepsilon_c)/d\varepsilon$, $dU(96, \varepsilon_c)/d\varepsilon$, and $dU(112, \varepsilon_c)/d\varepsilon$ in log $(dU)$ versus log$(l)$ coordinates. $\nu$ is obtained in a similar way, using $d(\log|d(\varepsilon_c|)/d\varepsilon, d(\log|d(\varepsilon_c|^2)/d\varepsilon$, and $d(\log|d(\varepsilon_c|^4)/d\varepsilon$; see Fig. 7b, second row from the top. $-\beta/\nu$ equals to the slope of linearly interpolated $\langle|d(64, \varepsilon_c)|\rangle$, $\langle|d(80, \varepsilon_c)|\rangle$, $\langle|d(96, \varepsilon_c)|\rangle$, and $\langle|d(112, \varepsilon_c)|\rangle$ in log$(\langle|d|\rangle)$ versus log$(l)$ scale. $\beta$ can also be calculated using $|d(\varepsilon_c)|^2$, or using $|d(\varepsilon_c)|^4$; see Fig. 7c, third row from the top. To get the ratio $-2\beta/\nu$ and $-4\beta/\nu$, $\langle|d|^2\rangle$ and $\langle|d|^4\rangle$ are used similarly as the $\langle|d|\rangle$ for the ratio $\beta/\nu$. $\gamma$ equals to the slope of linearly interpolated $\langle\chi(64, \varepsilon_c)\rangle$, $\langle\chi(80, \varepsilon_c)\rangle$, $\langle\chi(96, \varepsilon_c)\rangle$, and $\langle\chi(112, \varepsilon_c)\rangle$ in $log(\langle\chi\rangle)$ versus log$(l)$ scale; see Fig. 7d, bottom row.

Identity function $2\beta + \gamma = 2\nu$ holds for Ising systems. The error of this identity $I_{\text{error}}$ is used to verify the critical exponents estimation; see Table 2. We conclude that the critical exponents significantly deviate from each other and, in particular, from the Ising model. Parameters $\nu$ and $\gamma$ are decreasing, while $\beta$ and $\varepsilon_c$ are increasing, as the number of

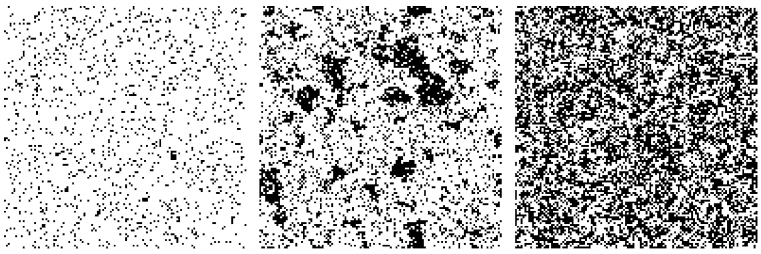

**(a)** Local model; $\varepsilon = 0.08, \varepsilon = 0.134, and \varepsilon = 0.25$

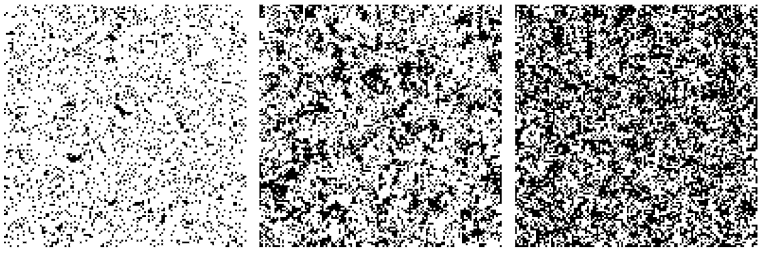

**(b)** Mixed model: $25\%(1)$ with $\varepsilon = 0.12, \varepsilon = 0.170, \varepsilon = 0.25$

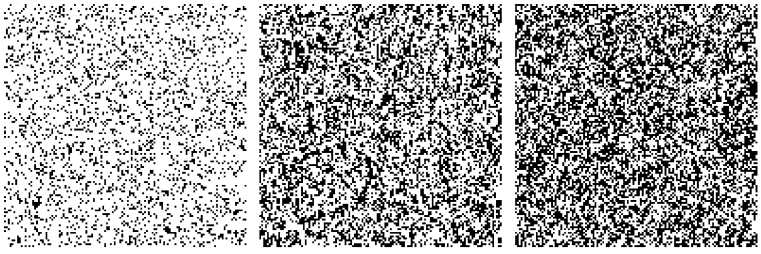

**(c)** Mixed model: $100\%(1)$ with $\varepsilon = 0.14, \varepsilon = 0.204, \varepsilon = 0.25$

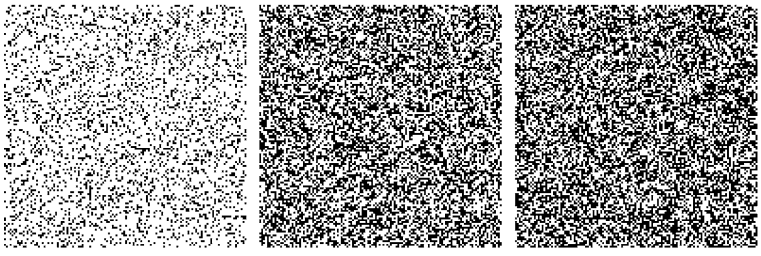

**(d)** Mixed model: $100\%(4)$ with $\varepsilon = 0.16, \varepsilon = 0.224, \varepsilon = 0.25$

**Fig. 6** The systems from top to bottom; **a** no remote neighbors; **b** 25% of sites have one remote neighbor 25%(1); all sites have one remote neighbor 100%(1); and all four neighbors are remote 100%(4)

remote connections increases. $\varepsilon_c$ is higher for systems with more nonlocal connections. Still, the identity function is satisfied in most cases with reasonable accuracy. It is expected that the somewhat larger errors can be further reduced if the number of iterations is increased.

## 4 Density of non-local links as critical parameter

In this section, we study the quantitative relationship between the density of non-local connections and critical probability $\varepsilon_c$. Previously we have observed that $\varepsilon_c$ increases as the density of remote connections increases. We have conducted a large number of experiments with various system configurations to quantify this relationship. In Fig. 8a–d, $\varepsilon_c$ is shown as a function of the proportion of sites with remote connections for many different systems. To calculate $\varepsilon_c$, we applied the same method as before. In the experiments in Fig. 8, we used shorter runs than previously, as less accuracy is sufficient if we do not aim at determining the critical exponents.

For a given number of remote links, usually there is a range of critical probabilities, depending on the actual way

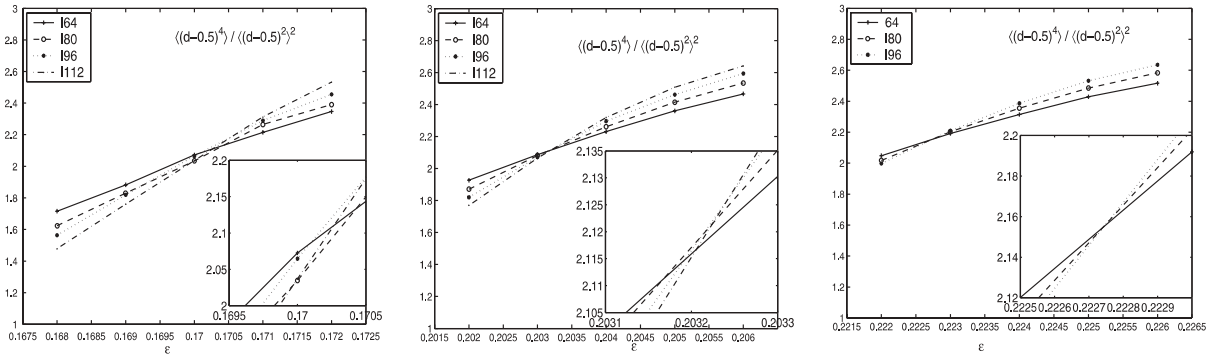


Estimation of the critical probability $\varepsilon_c$.

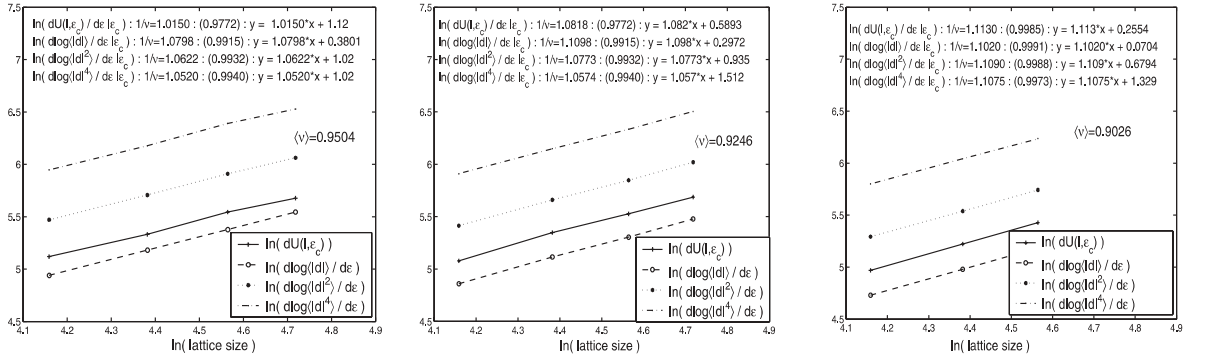


Estimation of the critical exponent of the correlation length $\nu$.

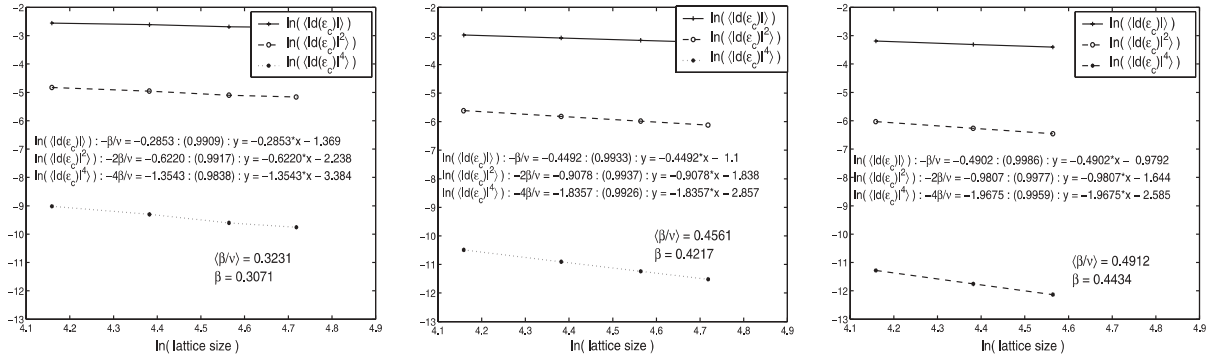


Estimation of the critical exponent of magnetization $\beta$.

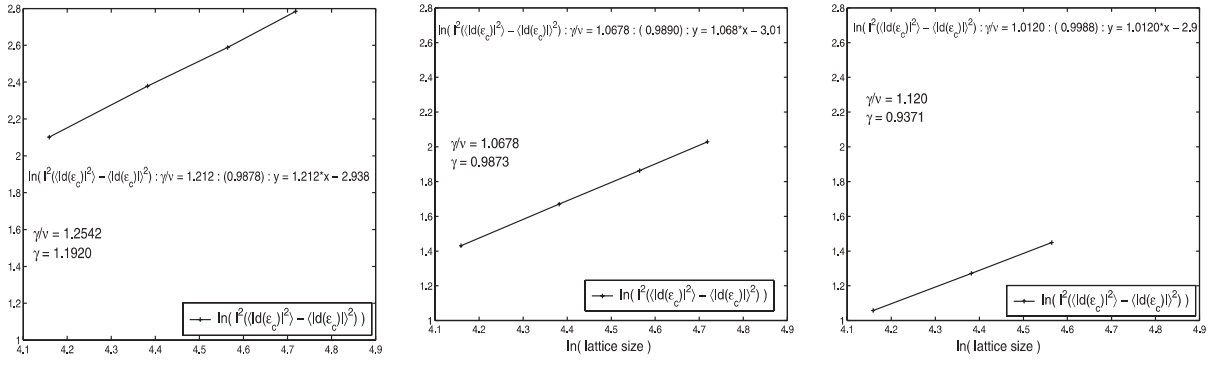


Estimation of the critical exponent of susceptibility $\gamma$.

**Fig. 7** Estimation of various critical parameters of mixed models using Binder's method of finite-size scaling. Experiments were conducted with $l \times l$ lattices of size $l$ = 64, 80, 96, and 112

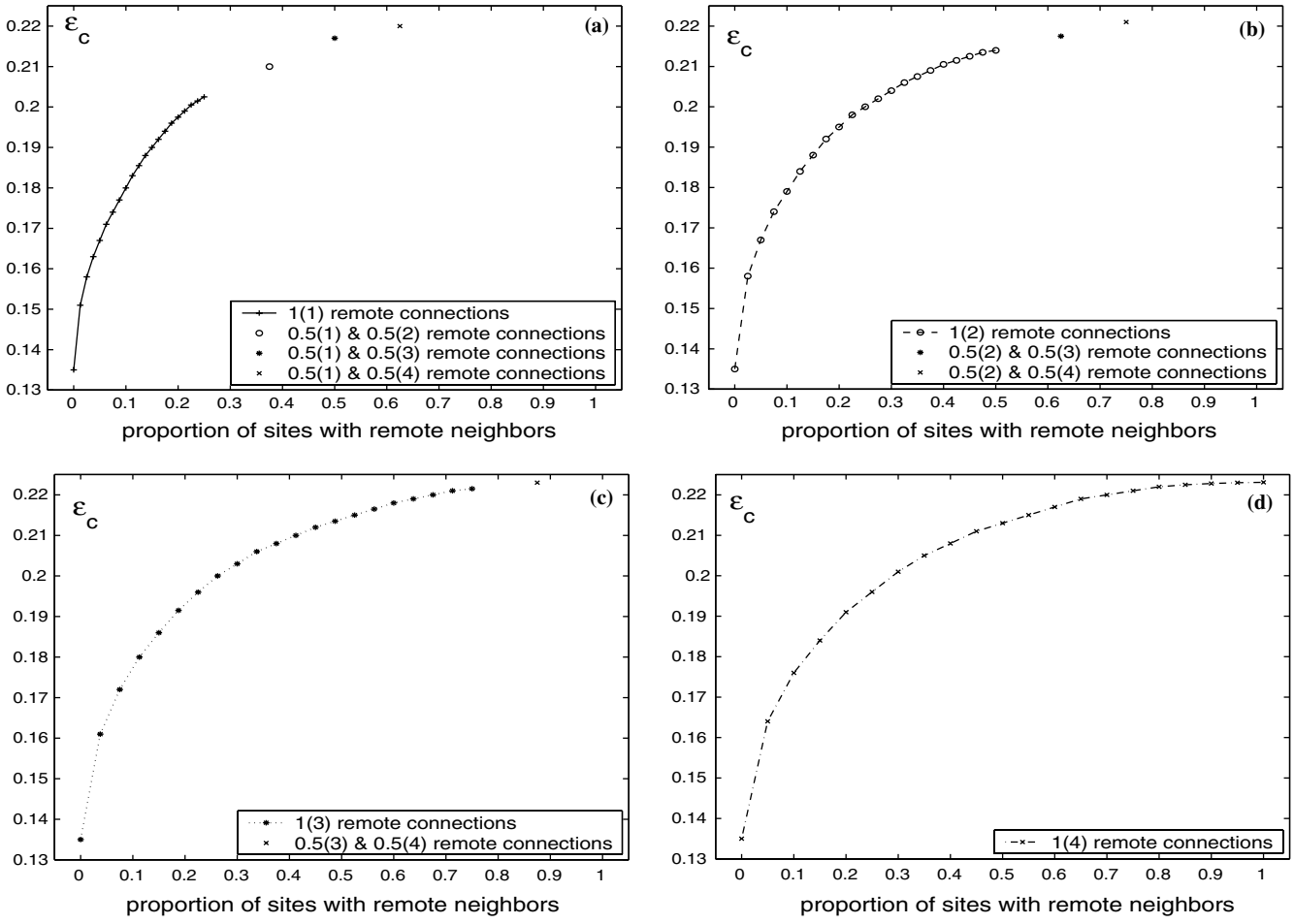


**Fig. 8** $\varepsilon_c$ as the function of the proportion of remote connections; **a** combinations of 50% of each 1 and 1, 1 and 2, 1 and 3, and 1 and 4 remote connections; **b** 50% of each 1 and 1, 2 and 3, and 2 and 4 remote connections; **c** 50% sites having 3 and 4 remote connections; **d** all sites have four remote connections

the connections are distributed. If the remote neighbors are evenly distributed among the neurons in the network, we get higher $\varepsilon_c$ values. At the same, time the $\varepsilon_c$ values are lower when the remote neighbors are clustered towards a fewer number of sites. It is concluded that the density of nonlocal connections acts as a critical parameter. Accordingly, by varying nonlocal connectivity while all other parameters of the system are fixed, we can produce critical behavior and phase transitions. This allows us to build phase diagrams in the state space of noise and nonlocality of interactions.

Such a phase diagram is shown in Fig. 9 where results obtained by various configurations are combined. Network structures with higher number of reciprocal remote connections make the system more vulnerable to disturbances, when the system evolution is governed by the random majority rule. One-way connections increase the network resistance to changes. In the case of only local or only remote neighbors, obviously we have only one configuration giving $\varepsilon_c$ values of 0.13428 and 0.2242, respectively.

## 5 Evolution of critical behavior in the neuropil

We propose the following hypothesis on the emergence of critical behavior with the potential of frequent phase transitions in the neuropil. The neural connectivity is sparse in the neuropil at the embryonic stage. Following birth, the connectivity increases and ultimately reaches a critical level, at which the neural activity becomes self-sustaining. The brain as a collective system is at the edge of criticality, and it now can undergo repeated phase transitions in a self-organized way, under the influence of external and internal factors. We suggest to implement this approach in a computational model as follows:

- Start with an initial population of nonlinear units, which model neural populations with given local properties;
- Incrementally increase the long-range connectivity using any desired strategy, producing, e.g., a scale-free network with preferential attachment, or other objects;

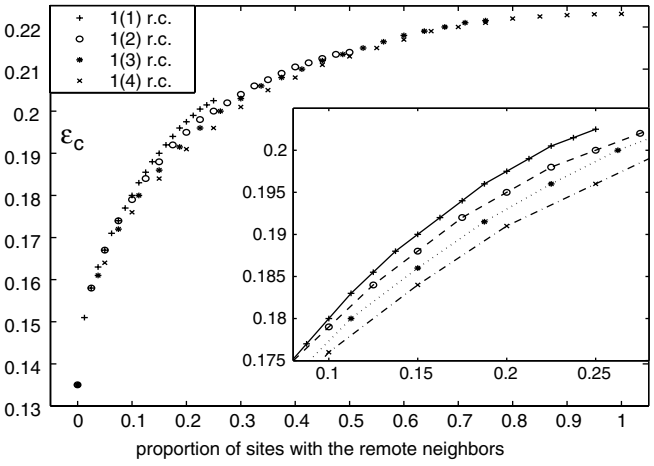


**Fig. 9** Integrated view of the relationship between critical noise and the proportion of remote connections for all studied network configurations

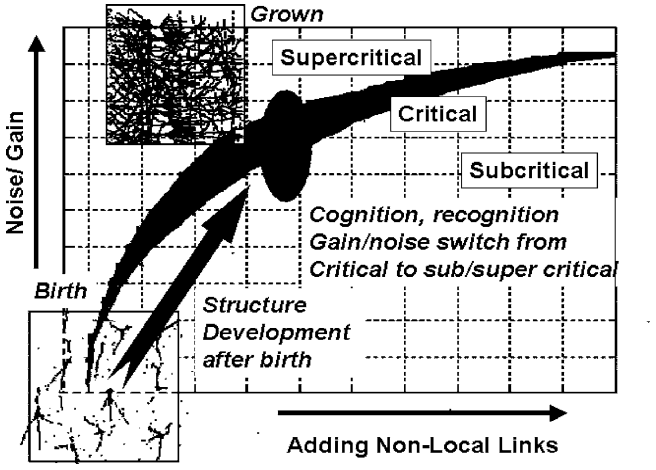


**Fig. 10** Illustration of self-organization of critical behavior in the percolation model of the neuropil

- Stop changing the connectivity when the critical state is approached. From this stage on, the structure is essentially fixed. Modifications still happens, e.g., due to learning effects;
- Use the effects of inputs and endogenous noise to balance the system at the edge of phase transitions during its operation;
- Operate the system through repeated phase transitions as it processes, retrieves, and transforms data.

The above strategy is schematically illustrated in Fig. 10. By way of structural evolution, the neuropil evolves toward regions of criticality or edge-of-criticality. Once the critical regions are established, the connectivity structure remains essentially unchanged. However, by adjusting the noise and/or gain levels, the system can be steered towards or away from critical regions. This is a control mechanism that provides the conditions to phase transitions in the neuropil. Obviously, the outlined mechanism is incomplete and in realistic neural systems, a host of additional factors play crucial role. However, the given mechanism is very robust and it may provide the required dynamical behavior in a wide range of real life conditions.

## 6 Conclusions

By describing certain topological and dynamical properties of the neuropil, we aim at modeling phase transitions in brains. Destabilization by sensory stimuli and sudden changes in the spatio-temporal neurodynamics in the cortex resembles phase transitions in physical systems. Phase transitions are much more complex in brains than in physics. In brains, transitions to a more organized phase are intermittent. The transition to the highly organized state happens in a matter of 3–5 ms. Multiple states commonly exist in both time and space in each cerebral hemisphere.

We suggested a novel method for modeling and functioning of the neuropil. The neuropercolation approach to phase transitions in the neuropil has the prospect of creating powerful, robust computational models that match the performance of neural systems. Our study identified key control parameters of this process, i.e., communication noise, and relative proportion of axonal connections. Phase diagrams were constructed and used to outline a hypothesis of self-organized development of the neuropil.

The postulated self-organization of behavior near the critical state assumes learning and adaptation in the system, as described in the previous section. The present random cellular automata, however, utilizes uniform weights between nodes, i.e., all nodes in a neighborhood are equally important. As a result, the system exhibits relatively simple dynamics with oscillations between two states. Clearly, learning effects will shape the attractor landscape and carve out evolved landscapes with multiple attractors. Adding learning effects is an important future task in building the hierarchy of dynamical memory models.

The proposed method of controlling phase transitions in the neuropil will be tested both in discrete neuropercolation models and in the continuous domain of K models, which use ordinary differential equations (Kozma and Freeman 2001) We explore the dynamics of spatio-temporal patterns in the neuropercolation model. In particular, we will study conditions that may lead to the emergence of phase cones and itinerant chaotic dynamics, as observed by brain monitoring methods.

**Acknowledgements** This research is supported by NSF grant EIA-0130352. Useful suggestions of the anonymous referee are highly appreciated.

## References

Aihara K, Takabe T, Toyoda M (1990) Chaotic neural networks. Phys Lett A 144(6–7):333–340

Aizeman M, Lebowitz JL (1988) Metastability effects in bootstrap percolation. J Phys A 21:3801–3813

Albert R, Barabási AL (2002) Statistical mechanics of complex networks. Rev Modern Phys 74:47
Arhem P, Blomberg C, Liljenstrom H (2000) Disorder versus order in brain function. In: Progr neural processing, Vol. 12, ISBN 981-02-4008-2, World Scientific, Singapore
Bak P (1996) How nature works - the science of self-organized criticality. Springer, Berlin Heidelberg New York
Bak P, Tang C, Wiesenfeld K (1987) Phys Rev Lett 59:381
Balister PN, Bollobás B, Stacey AM (1993) Upper bounds for the critical probability of oriented percolation in two dimensions. In: Proc Royal Soc Lond Ser A 440(1908):201–220
Balister P, Bollobás B, Kozma R (2004) Mean field models of probabilistic cellular automata. Random Struct Algorithms (on press)
Balister P, Bollobás B, Johnson R, Walters M (2003) Random majority percolation. (submitted)
Barabási L, Bonabeau E (2003) Scale-free networks. Sci Am 288:60–69
Barrie JM, Freeman WJ, Lenhart M (1996) Modulation by discriminative training of spatial patterns of gamma EEG amplitude and phase in neocortex of rabbits. J Neurophysiol 76:520–539
Berlekamp ER, Conway JH, Guy RK (1982) Winning ways for your mathematical plays, vol 1: games in general. Academic, New York
Binder K (1981) Finite scale scaling analysis of Ising model block distribution function. Z Phys B 43:119–140
Bollobás B (1985) Random Graphs. Academic, London
Bollobás B, Riordan O (2003) Results on scale-free random graphs. Handbook of graphs and networks, 1–34. Wiley-VCH, Weinheim
Bressler SL, Kelso JAS (2001) Cortical coordination dynamics and cognition. Trends Cogn Sci 5:26–36
Bressler SL (2002) Understanding cognition through large-scale cortical networks. Curr Directions Psychol Sci 11:58–61
Bressler SL (2003) Cortical coordination dynamics and the disorganization syndrome in schizophrenia. Neuropsychopharmacology 28:S35-S39
Cerf R, Cirillo EN (1999) Finite size scaling in three-dimensional bootstrap percolation. Ann Probab 27(4):1837–1850
Cipra BA (1987) An introduction to the ising model. Am Math Monthly 94:937–959
Crutchfield JP (1994) The calculi of emergence: computation, dynamics, and induction. Physica D 75:11–54
Dafilis MP, Liley DTJ, Cadusch PJ (2001) Robust chaos in a model of the electro-encephalogram: Implications for brain dynamics. Chaos 11:474–478
Duarte AMS (1989) Simulation of a cellular automaton with an oriented bootstrap rule. Physica A 157:1075–1079
Erdős P, Rényi A (1960). On the evolution of random graphs. Publ Math Inst Hung Acad Sci 5:17–61
Freeman WJ (1975) Mass action in the nervous system. Academic, New York
Freeman WJ (1999) Noise-induced first-order phase transitions in chaotic brain activity. Int J Bifurcation Chaos 9(11):2215–2218
Freeman WJ (2003a) The wave packet: an action potential for the 21st Century. J Integrative Neurosci 2:3–30
Freeman WJ (2003b) Evidence from human scalp EEG of global chaotic itinerancy. Chaos 13:1067–1077
Freeman WJ (2003c) A neurobiological theory of meaning in perception. Part 1. Information and meaning in nonconvergent and nonlocal brain dynamics. Int J Bifurc Chaos 13:2493–2511
Freeman WJ, Burke BC, Holmes MD (2003a) Aperiodic phase re-setting in scalp EEG of beta-gamma oscillations by state transitions at alpha-theta rates. Hum Brain Mapp 19:248–272
Freeman WJ, Burke BC, Holmes MD, Vanhatalo S (2003b) Spatial spectra of scalp EEG and EMG from awake humans. Clin Neurophysiol 114:1055–1060
Freeman WJ (2004) Origin, structure, and role of background EEG activity. Part 1. Analytic amplitude. Clin Neurophysiol 115:2077–2088
Friston KJ (2000) The labile brain. I. Neuronal transients and nonlinear coupling. Phil Trans R Soc Lond B 355:215–236
Gruber AJ, Solla SA, Surmeier DJ, Houk JC (2003) Modulation of striatal single units by expected reward: A spiny neuron model displaying dopamine-induced bistability. J Neurophysiol 90:1095–1114
Haken H (1999) What can synergetics contribute to the understanding of brain functioning? In: Uhl C (ed) Analysis of neurophysiological brain functioning. Springer, Berlin Heidelberg New York, pp 7-40
Gács P (1990) A Toom rule that increases the thickness of sets. J Statist Phys 59(1–2):171–193
Gravener J, McDonald E (1997) Bootstrap percolation in a polluted environment. J Statist Phys 87(3–4):915–927
Grimmett G (1999) Percolation in fundamental principles of mathematical sciences. Springer, Berlin Heidelberg New York *xiv*+444 pp
Hopfield JJ (1982) Neural networks and physical systems with emergent collective computational abilities. Proc Nat Acad Sci USA 79:2554–2558
Hoppensteadt FC, Izhikevich EM (1998) Thalamo-cortical interactions modeled by weakly connected oscillators: could the brain use FM radio principles? BioSystems 48:85–94
Ingber L (1995) Statistical mechanics of multiple scales of neocortical interactions. In: Nunez PL (ed) Neocortical dynamics and human EEG rhythms. Oxford, New York, pp 628–681
Jensen HJ (1998) Self-organized criticality – emergent behavior in physical and biological systems. Cambridge University Press, Cambridge
Kaneko K (1990) Clustering, coding, switching, hierarchical ordering, and control in a network of chaotic elements. Physica D 41:137–172
Kaneko K, Tsuda I (2001) Complex systems: chaos and beyond. A constructive approach with applications in life sciences
Kauffman SA (1990) Requirements for evolvability in complex systems: orderly dynamics and frozen components. Physica D 42:135–152
Korn H, Faure P (2003) Is there chaos in the brain? II. Experimental evidence and related models. Comptes Rendus Biologies 326:787–840
Kozma R (1998) Intermediate-range coupling generates low-dimensional attractors deeply in the chaotic region of one-dimensional lattices. Phys Lett A 244(1–3):85–91
Kozma R, Freeman WJ (2001) Chaotic resonance – methods and applications for robust classification of noisy and variable patterns. Int J Bifurcation Chaos 11:1607–1629
Kozma R, Balister P, Bollobás B, Freeman WJ (2001) Dynamical percolation models of phase transitions in the cortex In: Proceedings NOLTA 01 nonlinear theory and applications symposium, Miyagi, Japan, vol. 1, pp 55–59
Kozma R, Balister P, Bollobás B, Chen H, Freeman WJ (2003) Analysis of scaling laws in a local random cellular automata model (submitted)
Kozma R, Puljic M, Balister P, Bollobás B, Freeman WJ (2004) Neuropercolation: a random cellular automata approach to spatio-temporal neurodynamics. Lecture Notes Computer Science LNCS vol 3350, Springer, Berlin Heidelberg New York, pp 435–443
Linkenkaer-Hansen K, Nikouline VM, Palva JM, Iimoniemi RJ (2001) Long-range temporal correlations and scaling behavior in human brain oscillations. J Neurosci 15:1370–1377
Maes C, Vande Velde K (1997) Relative energies for non-Gibbsian states. Comm Math Phys 189(2):277–286
Makowiec D (1999) Stationary states for Toom cellular automata in simulations. Phys Rev E 55:3795
Marcq P, Chaté H, Manneville P (1997) Universality in Ising-like phase transitions of lattices of coupled chaotic maps. Phys Rev E 55(3):2606–2627
Newman MEJ (2000) Models of the small world. J Stat Phys 101:819–841
Ohl FW, Scheich H, Freeman WJ (2001) Change in pattern of ongoing cortical activity with auditory category learning. Nature 412:733–736
Ohl FW, Deliano M, Scheich H, Freeman WJ (2003) Early and late patterns of stimulus-related activity in auditory cortex of trained animals. Biol Cybern 88:374–379
Peters A, Palay SL, deF H (1991) Webster fine structure of the nervous system: neurons and their supporting cells. Oxford University Press, Oxford)

Pomeau Y (1993) Periodic behavior in cellular automata. J Stat Phys 70(5–6):1379–1382
Puljic M, Kozma R, (2003) Phase transitions in a probabilistic cellular neural network model having local and remote connections. IEEE/INNS International Joint Conference Neural Network IJCNN'2003, pp 831–835
Puljic M, Kozma R (2005) Activation clustering in neural and social networks. Complexity (in press)
Schiff SJ et al (1994) Controlling chaos in the brain. Nature 370:615–620
Skarda CA, Freeman WJ (1987) How brains make chaos in order to make sense of the world. Behav Brain Sci 10:161–195
Stam CJ, Breakspear M, van Cappellen van Walsum A-M, van Dijk BW (2003) Nonlinear synchronization in EEG and whole-head recordings of healthy subjects. Hum Brain Mapp 19:63–78
Stauffer D, Aharony A (1994) Introduction to percolation theory. Selwood Printing Ltd, West Sussex
Toom AL, Vasilyev NB, Stavskaya ON, Mityushin LG, Kurdyumov GL, Prigorov SA (1990) Discrete local Markov systems in Stochastic cellular systems:ergodicity, memory, morphogenesis. In: Dobrushin RL, Kryukov VI, Toom AL (eds) Nonlinear Science: theory and applications. Manchester University Press, UK
Wang XF, Chen GR (2003) Complex networks: small-world, scale-free and beyond. IEEE Trans Circuits Syst 31:6–20
Watts DJ, Strogatz SH (1998) Collective dynamics of small-world networks. Nature 393:440–442